Theoretical Study of the Water-Assisted Aminolysis of β-Lactams: Implications for the Reaction between Human Serum Albumin and Penicillins

Natalia Díaz,[†] Dimas Suárez,[‡] and Tomás L. Sordo*,[†]

Contribution from the Departamento de Química Física y Analítica, Universidad de Oviedo, Julián Clavería 8, 33006 Oviedo, Spain, and Department of Chemistry, Eberly College of Sciences, The Pennsylvania State University, 152 Davey Laboratory, University Park, Pennsylvania 16802-6300

Received October 4, 1999. Revised Manuscript Received April 11, 2000

Abstract: The ring opening of 2-azetidinone via a neutral H_2O-assisted aminolysis process is studied using different quantum chemical methods (MP2/6-31G**, B3LYP/6-31G**, and G2(MP2,SVP) levels of theory) as a further step to the theoretical investigation of the aminolysis reaction of β-lactam antibiotics (Díaz, N.; Suárez, D.; Sordo, T. L. *Chem. Eur. J.* **1999**, *5*, 1045−1054; Díaz, N.; Suárez, D.; Sordo, T. L. *J. Org. Chem.* **1999**, *64*, 9144−9152). The calculated pathways are analogous to those previously described for the amine-assisted aminolysis reaction, a syn stepwise mechanism being the most favored one both in the gas phase and in solution with an energy barrier of around 39.7 kcal/mol ($\Delta G_{solution}$). For this process the strong catalytic action of one water molecule amounts to 23.0 (G2(MP2,SVP) electronic energy), 12.6 ($\Delta G_{gas-phase}$), and 9.1 kcal/mol ($\Delta G_{solution}$). The water-assisted reaction between methylamine and the 3α-carboxypenam anion was also studied at the B3LYP/6-31+G* level of theory to model the specific role of water in the aminolysis of bicyclic β-lactam antibiotics. For this system the most favorable attack of CH_3NH_2 to the carbonylic group in a low polar media can occur through simultaneous H-transfer to the carboxylate group assisted by the ancillary water molecule with a $\Delta G_{gas\ phase}$ barrier of 31.0 kcal/mol with respect to separate reactants. A concerted route becomes the most favored mechanism for the aminolysis of penicillins assisted by an ancillary water molecule in aqueous solution. The structure of the concerted transition state is in agreement with the experimentally reported Brønsted β-values close to unity. Interestingly, according to the experimental structure of the Lys_{199} active center of Human Serum Albumin, the mechanism for the aminolysis reaction of β-lactams in a protein environment may be similar to the stepwise route found in the gas phase for 3α-carboxypenam.

Introduction

Before reaching their biological receptors, molecules of physiologically active compounds normally interact with blood plasmid proteins to form weak or covalent complexes. This is the case of the penicilloyl groups formed by reaction between lysine residues in plasmid proteins and penicillin, which is considered the major antigenic determinant of penicillin allergy detected by the immune system.[1]

The Human Serum Albumins (HSAs) are the major soluble protein constituents of the circulatory system, and hence are involved in the transport, distribution, and metabolism of many endogenous ligands (fatty acids, bilirubin, amino acids, metals, etc.) and numerous pharmaceuticals as well.[2] In view of its abundance in the human plasma and its functioning as a carrier protein, recent experimental studies have focused on the binding of penicillins to HSA.[3] Several benzylpenicilloyl-containing peptides have been identified in different binding regions of HSA involving six different lysine residues. Particularly, one of these groups, Lys_{199}, is also an important binding residue for other compounds such as acetylsalicylic acid, triodobenzoic acid, etc.

To further understand the biochemical activity of these antibiotics, the reaction of β-lactams with amines in aqueous solution has been extensively studied.[4−8] For a series of primary monoamines, it has been found experimentally that the importance of the different terms contributing to the observed pseudo-first-order rate constant for the disappearance of the β-lactam compounds **1**−**3** in Scheme 1 depends on the basicity and concentration of the amine and the pH.[5−8]

Thus, at high pH the aminolysis reaction of β-lactams **1**−**3** proceeds predominantly via the specific hydroxide-catalyzed pathway while the kinetic constants on $[RNH_2]$ and $[RNH_2]$,[2] corresponding to the uncatalyzed and the amine-catalyzed aminolysis, respectively, are the predominant terms when weakly

[†] Universidad de Oviedo.

[‡] The Pennsylvania State University. On leave from Universidad de Oviedo, Spain.

(1) Levine, B. B.; Ovary, Z. *J. Exp. Med.* **1961**, *114*, 875−904.

(2) Peters, T. *All about Albumin: Biochemistry, Genetics and Medical Applications*; Academic Press: San Diego, 1996.

(3) (a) Nerli, B.; Romanin, D.; Picó, G. *Chem.-Biol. Interact.* **1997**, *104*, 179−202. (b) Yvon, M.; Anglade, P.; Val. J. M. *FEBS Lett.* **1990**, *263*, 237−240. (c) Yvon, M.; Anglade, P.; Val. J. M. *FEBS Lett.* **1989**, *247*, 273−278. (d) Yvon, M.; Anglade, P.; Val. J. M. *FEBS Lett.* **1988**, *239*, 237−240.

(4) (a) Page, M. I. *Acc. Chem. Res.* **1984**, *17*, 144−151. (b) Page. M. I. The mechanism of Reactions of β-lactams. In *The Chemistry of β-lactams*; Page, M. I., Ed.; Blackie Academic & Professional: London, 1992; pp 129−147. (c) Georg, G. I.; Ravikumar, V. T. *The Organic Chemistry of β-Lactams*; Georg, V. T., Ed.; VCH Publishers: New York, 1993.

(5) Gensmantel, N. P.; Page, M. I. *J. Chem. Soc., Perkin Trans. 2* **1979**, 137−142.

(6) (a) Morris, J. J.; Page, M. I. *J. Chem. Soc., Perkin Trans. 2* **1980**, 212−219. (b) Morris, J. J.; Page, M. I. *J. Chem. Soc., Perkin Trans. 2* **1980**, 220−224.

(7) Blackburn, G. M.; Plackett, J. D. *J. Chem. Soc., Perkin Trans. 2* **1973**, 981−985.

(8) Yamana, T.; Tsuji, A.; Miyamoto, E.; Mira, E. *J. Pharm. Pharmac.* **1975**, *27*, 56−57.

10.1021/ja993547q CCC: $19.00
Published on Web 06/29/2000

Scheme 1

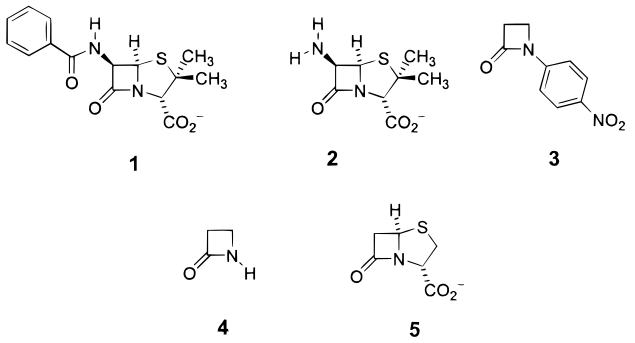

Scheme 2

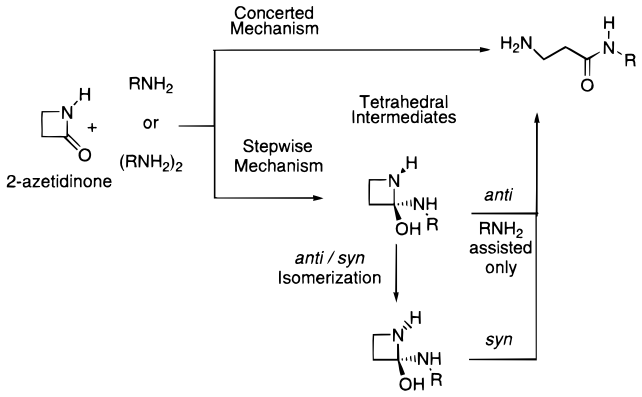

basic amines react with β-lactams in the biologically relevant pH range 6−8. Kinetic experiments[5−8] have been interpreted in terms of a stepwise mechanism through *zwitterionic* intermediates for the aminolysis of β-lactams.[4] In particular, Brønsted plots for the kinetic constants for the uncatalyzed aminolysis of **1**−**3** give slopes close to unity suggesting that a positive charge is developed on the amine N atom at the rate-determining transition structures.[5,7] However, the specific role that solvent molecules could play in the mechanism of aminolysis of β-lactams has not been clarified by experiments.

To gain some theoretical insight into the thermal and amine-assisted aminolysis of β-lactams, we have previously studied the ring opening of the simplest β-lactam, 2-azetidinone **4**, by the reaction with either RNH_2 or the RNH_2 dimer (R = H, CH_3).[9−11] For these processes the ring opening of 2-azetidinone may occur via a concerted mechanism or via stepwise pathways passing through various neutral tetrahedral intermediates (see Scheme 2).

The most favorable pathway for both the thermal[9] and RNH_2-assisted[10,11] processes is a stepwise mechanism that begins with a nucleophilic attack of RNH_2 to the carbonyl group leading to a neutral tetrahedral intermediate in which the attacking group and the N lone pair have a synperiplanar relationship (see Scheme 2). For the monocyclic model system, 2-azetidinone, this preferential orientation stems only from electronic factors.[9] The most favorable evolution of the intermediate proceeds through an *anti/syn* isomerization followed by H-transfer between the hydroxyl and the forming amino group with simultaneous cleavage of the β-lactam ring (see Scheme 2). Interestingly, for bicyclic systems such as 3α-carboxypenam **5**, in which the *anti/syn* isomerization is impeded, theoretical calculations[12] have shown that the most favored mechanism for aminolysis in aqueous solution may be the concerted one in contrast with earlier proposals.[4]

From the previous theoretical and experimental work on the aminolysis of β-lactams,[4−12] it is clear that a computational examination of the catalytic role played by an ancillary water molecule may improve our understanding of these processes. In the present work, we report a quantum chemical study of the water-catalyzed reactions between methylamine and two β-lactam models: 2-azetidinone **4** and the 3α-carboxypenam anion **5**. This study will allow the specific effect produced by a solvent molecule on these processes to be displayed. To discuss the feasibility of the mechanisms found for the aminolysis of β-lactams in a protein environment, we will analyze the Lys_{199} binding site of HSA using the crystallographic coordinates available[13] and discuss the possible interactions between benzylpenicillin and this binding site. This analysis could afford us further insight into the biochemical processes taking place in allergic reactions to penicillins.

Methods

Quantum chemical calculations were carried out with the Gaussian 94 and Gaussian 98 systems of programs.[14] For the reaction of 2-azetidinone, stable structures were fully optimized and Transition Structures (TSs) located at the MP2/6-31G** and B3LYP/6-31G** levels.[15,16] All the critical points were further characterized by analytic computation of harmonic frequencies at the B3LYP/6-31G** level. Thermodynamic data (298 K, 1 bar) were computed using B3LYP/6-31G** frequencies within the ideal gas, rigid rotor, and harmonic oscillator approximations.[17]

To estimate the effect of larger basis sets and the more elaborated *N*-electron treatments on the relative energies, electronic energies were also computed for all the MP2/6-31G** optimized structures using a modified version of the G2(MP2,SVP) scheme.[18] To save a considerable amount of the computational cost of the QCISD(T)/6-31G* calculations by reducing by 19 the number of basis functions, we assumed a formal

(9) Díaz, N.; Suárez, D.; Sordo, T. L. *Chem. Eur. J.* **1999**, *5*, 1045−1054.
(10) Díaz, N.; Suárez, D.; Sordo, T. L. *J. Org. Chem.* **1999**, *64*, 3281−3289.
(11) Díaz, N.; Suárez, D.; Sordo, T. L. *J. Org. Chem.* **1999**, *64*, 9144−9152.
(12) Díaz, N.; Suárez, D.; Sordo, T. L. *Chem. Eur. J.* Manuscript submitted for publication.
(13) (a) He, X. M.; Carter, D. C. *Nature* **1992**, *358*, 209−215, PDB ID code 1UOR. (b) Sugio, S.; Mochizuki, S.; Noda, M.; Kashima, A. *Protein Eng.* **1999**, *12*, 439−446, PDB ID code 1AO6. (c) Curry, S.; Mandeikow, H.; Brick, P.; Franks, N. *Nature Struct. Biol.* **1998**, *5*, 827−835, PDB ID code 1BKE.
(14) (a) Frisch, M. J.; Trucks, G. W.; Schlegel, H. B.; Gill, P. M. W.; Johnson, P. M. W.; Robb, M. A.; Cheeseman, J. R.; Keith, T.; Petersson, G. A.; Montgomery, J. A.; Raghavachari, K.; Al-Laham, M. A.; Zakrzewski, V. G.; Ortiz, J. V.; Foresman, J. B.; Peng, C. Y.; Ayala, P. Y.; Chen, W.; Wong, M. W.; Andres, J. L.; Replogle, E. S.; Gomperts, R.; Martin, R. L.; Fox, D. J.; Binkley, J. S.; Defrees, D. J.; Baker, J.; Stewart, J. P.; Head-Gordon, M.; Gonzalez, C.; Pople, J. A. *Gaussian 94*; Gaussian, Inc.: Pittsburgh, PA, 1995. (b) Frisch, M. J.; Trucks, G. W.; Schlegel, H. B.; Scuseria, G. E.; Robb, M. A.; Cheeseman, J. R.; Zakrzewski, V. G.; Montgomery, J. A.; Stratmann, R. E., Jr.; Burant, J. C.; Dapprich, S.; Millam, J. M.; Daniels, A. D.; Kudin, K. N.; Strain, M. C.; Farkas, O.; Tomasi, J.; Barone, V.; Cossi, M.; Cammi, R.; Mennucci, B.; Pomelli, C.; Adamo, C.; Clifford, S.; Ochterski, J.; Petersson, G. A.; Ayala, P. Y.; Cui, Q.; Morokuma, K.; Malick, D. K.; Rabuck, A. D.; Raghavachari, K.; Foresman, J. B.; Cioslowski, J.; Ortiz, J. V.; Stefanov, B. B.; Liu, G.; Liashenko, A.; Piskorz, P.; Komaromi, I.; Gomperts, R.; Martin, R. L.; Fox, D. J.; Keith, T.; Al-Laham, M. A.; Peng, C. Y.; Nanayakkara, A.; Gonzalez, C.; Challacombe, M.; Gill, P. M. W.; Johnson, B.; Chen, W.; Wong, M. W.; Andres, J. L.; Gonzalez, C.; Head-Gordon, M.; Replogle, E. S.; Pople, J. A. *Gaussian 98, Revision A.6*; Gaussian, Inc.: Pittsburgh, PA, 1998.
(15) Hehre, W. J.; Radom, L.; Pople, J. A.; Schleyer, P. v. R. *Ab Initio Molecular Orbital Theory*; John Wiley & Sons Inc.: New York, 1986.
(16) (a) Becke, A. D. *J. Chem. Phys.* **1993**, *98*, 5648−5652. (b) Becke, A. D. *Phys. Rev. A* **1988**, *38*, 3098−3100. (c) Lee, C.; Yang, W.; Parr, R. G. *Phys. Rev. B* **1988**, *37*, 785−789.
(17) McQuarrie, D. A. *Statistical Mechanics*; Harper & Row: New York, 1976.
(18) Curtiss, L. A.; Redfem, P. C.; Smith, B. J.; Radom, L. *J. Chem. Phys.* **1996**, *104*, 5148−5152.

partition of the QCISD(T)/6-31G* contributions by decomposing it into two terms corresponding to a QCISD(T)/6-31G* calculation (estimated after having replaced the methyl group by one H atom using a standard N−H bond length of 1.01 Å) and a MP2/6-31G* term accounting for a formal isodesmic reaction step to consider the methyl effects. We have already shown[11] that the absolute error due to this approximation is substantially lower than the average absolute deviation of the G2(MP2,SVP) method (1.63 kcal/mol).

The main TSs for the H_2O-assisted aminolysis of 2-azetidinone were analyzed carrying out a Configurational Analysis (CA).[19] This interpretative tool rewrites a TS monodeterminantal wave function (built in this work from the B3LYP/6-31G** MOs[20]) as a combination of the electronic configurations of the interacting fragments, obtaining thus a more chemically graspable picture of the catalytic effect of the water molecule. This analysis was performed using a revised version of the ANACAL program.[21] In addition the electrostatically derived atomic charges at the B3LYP/6-31G** level were also computed according to the Merz−Kollman−Singh scheme.[22]

We note that the computational and interpretative procedures described above provide results which are readily comparable with those for the uncatalyzed and RNH_2-assisted aminolysis of 2-azetidinone previously studied.[9−11]

Owing to the size of the 3α-carboxypenam anion, the B3LYP/6-31+G* level of theory was used to study the water-assisted aminolysis of this bicyclic system, including diffuse functions in the basis set, to get an appropriate description of the negatively charged species.[23] This level of theory was calibrated by studying the Potential Energy Surface for the ammonolysis of a prototype system (2-formamide-acetate) at the B3LYP/6-31+G* and MP2/6-31+G* levels of theory. For the MP2/6-31+G* optimized structures, electronic energies were recalculated using the G2(MP2,SVP) scheme. By carrying out a comparative analysis, we found that the B3LYP/6-31+G* level of theory is adequate to study the aminolysis of the 3α-carboxypenam anion (see Results and Discussion in the text and Supporting Information). All of the critical structures involved in the aminolysis of 3α-carboxypenam were characterized and thermodynamical data were calculated from the corresponding B3LYP/6-31+G* frequency calculations.

To take into account condensed-phase effects on the kinetics and thermodynamics, quantum chemical computations on solvated structures were carried out by means of a Self-Consistent-Reaction-Field (SCRF) model.[23] The solvent is represented by a continuum characterized by a relative static dielectric permittivity of 78.3 to simulate water as the solvent used in the experimental work. The solute, which is placed in a cavity created in the continuum after spending some cavitation energy, polarizes the continuum, which in turn creates an electric field inside the cavity. This interaction can be taken into account using quantum chemical methods by minimizing the electronic energy of the solute plus the electrostatic Gibbs energy change corresponding to the solvation process that is given by:

$$\Delta G_{\text{solvation}} = -{}^1/_2 E_{\text{int}}$$

where E_{int} is the solute−solvent interaction energy:

$$E_{\text{int}} = \sum_{\alpha} V_{\text{el}}(\mathbf{R}_\alpha) Z_\alpha - \int V_{el}(\mathbf{r})\, \rho(\mathbf{r})\, \mathrm{d}\mathbf{r}$$

In this equation, V_{el} is the electrostatic potential created by the polarized continuum in the cativy, $\mathbf{R}_\alpha$ and Z_α are the position vector and charge of the nucleus α, respectively, and $\rho(\mathbf{r})$ is the electronic charge density at point $\mathbf{r}$. The factor $-{}^1/_2$ arises in the Gibbs energy from the fact that the positive work required to polarize the medium is exactly one-half the value of the interaction energy in the linear response approximation.[23] Addition to $\Delta G_{\text{gas phase}}$ of the solvation Gibbs energy, evaluated neglecting the change in the relative value of the thermal corrections when going from a vacuum to the solution, gives $\Delta G_{\text{solution}}$.

Different approaches can be followed to calculate the electrostatic potencial V_{el}. For the aminolysis of 2-azetidinone and the 3α-carboxypenam anion, the recently derived UAHF (united atom Hartree−Fock) parametrization[24d] of the polarizable continuum model[26] (PCM) was used, including both electrostatic and nonelectrostatic solute−solvent interactions. The solvation Gibbs energies $\Delta G_{\text{solvation}}$ along the reaction coordinate were evaluated from single-point PCM-UAHF calculations at the MP2/6-31G** level for 2-azetidinone and at the B3LYP/6-31+G* level for 3α-caboxypenam.[14b] The SCRF calculations were carried out on the gas-phase geometries given that previous work on the uncatalyzed aminolysis reaction has rendered similar optimized geometries both in the gas phase and in solution.[9]

To obtain results directly comparable with previous ones on the thermal and RNH_2-catalyzed aminolysis of 2-azetidinone,[9−11] the calculation of V_{el} for the H_2O-assisted aminolysis of 2-azetidinone was also performed at the MP2/6-31G** level of theory using the solvation model developed by Rivail and co-workers at the University of Nancy.[24] This SCRF method employs a monocentric multipolar expansion of the molecular charge distribution to compute the solute−solvent interaction energy and assumes a general cavity shape that is obtained using van der Waals solute atomic spheres with modified radii ($1.3084 r_{\text{vdW}}$),[23a] necessary to fulfill the volume condition.

Results and Discussion

We present first the results corresponding to the water-assisted aminolysis of 2-azetidinone, then those for the 3α-carboxypenam anion, and finally, we discuss the interaction between benzylpenicillin and a model of the Lys_{199} binding site in HSA.

Water-Assisted Aminolysis Reaction of 2-Azetidinone The exploration of the Potential Energy Surface (PES) for the neutral aminolysis of 2-azetidinone catalyzed by a water molecule rendered three possible pathways starting from two different prereactive complexes: a concerted one and two stepwise ones, the *anti* and the *syn* mechanisms. These pathways are analogous to those previously described for the RNH_2-assisted aminolysis reaction.[10,11]

The optimized geometries of the main TSs located along the concerted and stepwise reaction paths are shown in Figure 1. Table 1 collects the relative energies along the reaction profiles obtained at the different levels of theory. The $\Delta G_{\text{gas phase}}$ values in Table 1 combine the G2(MP2,SVP) electronic energies and the thermal corrections from the B3LYP/6-31G** analytical frequencies. As already mentioned, $\Delta G_{\text{solvation}}$ for 2-azetidinone was calculated at the MP2/6-31G** level using both the PCM-UAHF model and the multipolar expansion model (Nancy model). The two series of $\Delta\Delta G_{\text{solvation}}$ values in Table 1 are qualitatively similar and predict that the energy profiles with respect to reactants are destabilized in solution. The PCM-UAHF model produces a destabilization which is about 3−6 kcal/mol greater than that of the Nancy model. Addition of the MP2/

(19) (a) Fujimoto, H.; Kato, S.; Yamabe, S.; Fukui, K. *J. Chem. Phys.* **1974**, *60*, 572−578. (b) Menéndez, M. I.; Sordo, J. A.; Sordo, T. L. *J. Phys. Chem.* **1992**, *96*, 1185−1187.

(20) Stowasser, R.; Hoffmann, R. *J. Am. Chem. Soc.* **1999**, *121*, 3414−3420.

(21) López, R.; Menéndez, M. I.; Suárez, D.; Sordo, T. L.; Sordo, J. A. *Comput. Phys. Commun.* **1993**, *76*, 235−249.

(22) (a) Besler, B. H.; Merz, K. M.; Kollman, P. A. *J. Comput. Chem.* **1990**, *11*, 431−439. (b) Singh, U. C.; Kollman, P. A. *J. Comput. Chem.* **1984**, *5*, 129−145.

(23) (a) Clark, T.; Chandrasekhar, J.; Spitznagel, G. W.; Schleyer, P. v. R. *J. Comput. Chem.* **1983**, *4*, 294−301. (b) Gill, P. M. W.; Johnson, B. G.; Pople, J. A.; Frisch, M. J. *Chem. Phys. Lett.* **1992**, *197*, 499−505.

(24) (a) Rivail, J. L.; Rinaldi, D.; Ruiz-López, M. F. In *Theoretical and Computational Model for Organic Chemistry*; Formosinho, S. J., Csizmadia, I. G., Arnaut, L., Eds.; NATO ASI Ser. C; Kluwer Academic Publishers: Dordrecht, 1991; Vol. 339, pp 79−92. (b) Dillet, V.; Rinaldi, D.; Angyán, J. G.; Rivail, J. L. *Chem. Phys. Lett.* **1993**, *202*, 18−22. (c) Dillet, V.; Rinaldi, D.; Rivail, J. L. *J. Phys. Chem.* **1994**, *98*, 5034−5039. (d) Claverie, P. In *Quantum Theory of Chemical Reactions*; Daudel, R., Pullman, A., Salem, L., Veillard, A., Eds.; Reidel: Dordrecht, 1982; Vol. 3, pp 151−175.

(25) Barone, V.; Cossi, M.; Tomasi, J. *J. Chem. Phys.* **1997**, *107*, 3210−3221.

(26) Tomasi, J.; Persico, M. *Chem. Rev.* **1994**, *94*, 2027−2094. (b) Tomasi, J.; Cammi, R. *J. Comput. Chem.* **1995**, *16*, 1449−1458.

Table 1. Relatives Energies[a] (kcal/mol) with Respect to Reactants of the Structures Considered in the Aminolysis Reaction of 2-azetidinone Assisted by H_2O

structures	B3LYP/6-31G**	MP2/6-31G**	G2(MP2,SVP)[b]	$\Delta G_{\text{gas phase}}$[c]	$\Delta\Delta G_{\text{solvation}}$[d]	$\Delta G_{\text{solution}}$[e]
$CH_3NH_2 + H_2O$ + 2-azetidinone	0.0	0.0	0.0	0.0	0.0 (0.0)	0.0
$\mathbf{C_C}$	−8.2	−10.2	−6.4	11.3	0.4[f] (11.2)	11.7
$\mathbf{TS_C}$	18.1	14.7	19.8	41.1	3.9 (6.7)	45.0
$\mathbf{P_C}$	−27.2	−31.3	−28.1	−9.4	5.9 (9.6)	−3.5
$\mathbf{C_S}$	−12.4	−14.1	−10.7	6.5	8.0 (13.4)	14.5
$\mathbf{TS_1}$	13.5	8.6	13.5	35.4	4.4 (9.2)	39.7
$\mathbf{I_1}$-***anti***	−0.6	−7.9	−4.4	16.6	7.2 (12.5)	23.8
$\mathbf{TS_2}$-***anti***	28.4	22.7	29.2	51.6	5.9 (10.2)	57.5
$\mathbf{P_S}$	−31.8	−34.5	−31.0	−11.9	4.5 (10.4)	−7.4
$\mathbf{TS_i}$	4.8	−0.6	1.6	22.7	6.4 (11.3)	29.1
$\mathbf{I_2}$-***syn***	2.4	−4.3	−2.0	19.0	5.0 (9.2)	24.0
$\mathbf{TS_H}$	3.0	−3.4	−0.5	21.2	6.4 (10.7)	27.6
$\mathbf{I_3}$-***syn***	−0.3	−7.4	−4.3	16.6	7.9 (11.8)	24.5
$\mathbf{TS_2}$-***syn***	10.4	6.2	10.4	32.2	5.6 (9.4)	37.8
H_2O + 3-amino-*N*-methylpropanamide	−25.0	−28.1	−26.5	−14.9	1.9 (4.1)	−13.0

[a] Including ZPVE correction from B3LYP/6-31G** frequencies. [b] Single-point calculations on MP2/6-31G** geometries. [c] G2(MP2,SVP) electronic energies and B3LYP/6-31G** thermal corrections. [d] MP2/6-31G** SCRF solvation energies employing a monocentric multipolar expansion. Values in parentheses correspond to the MP2/6-31G** PCM-UAHF solvation energies. [e] Including MP2/6-31G** SCRF solvation energies employing a monocentric multipolar expansion. [f] For $\mathbf{C_C}$ the monocentric multipolar expansion of $\Delta G_{\text{solvation}}$ shows a poor convergence.

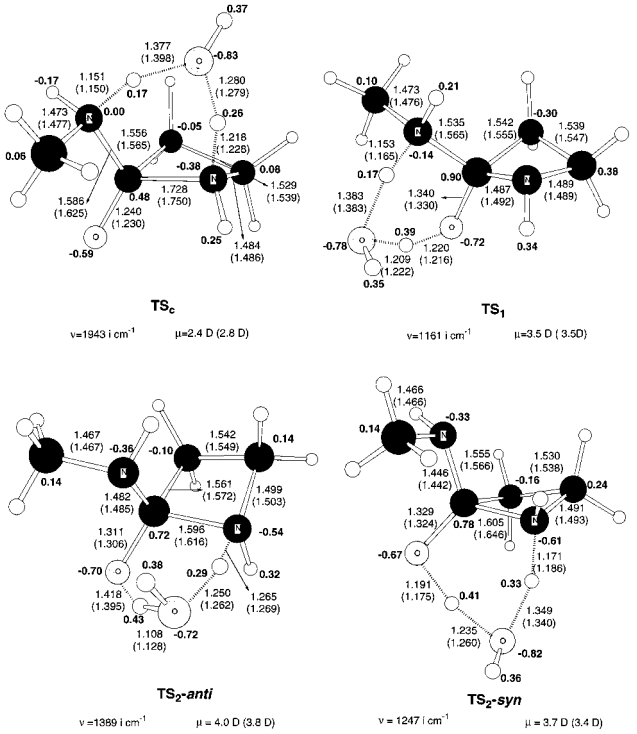

Figure 1. MP2/6-31G** and B3LYP/6-31G** (in parentheses) optimized structures for the main TSs for the H_2O-assisted aminolysis reaction of 2-azetidinone. Distances in Å. B3LYP/6-31G** MKS atomic charges in bold characters. Dipole moments (in Debyes) and frequencies corresponding to the transition vectors are also displayed.

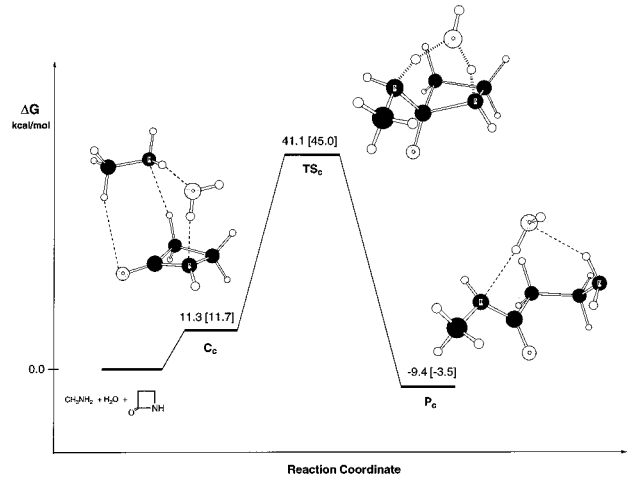

Figure 2. Gibbs energy profiles (kcal/mol) both in the gas phase and in solution (in brackets) for the concerted reaction channel corresponding to the H_2O-assisted aminolysis reaction of 2-azetidinone.

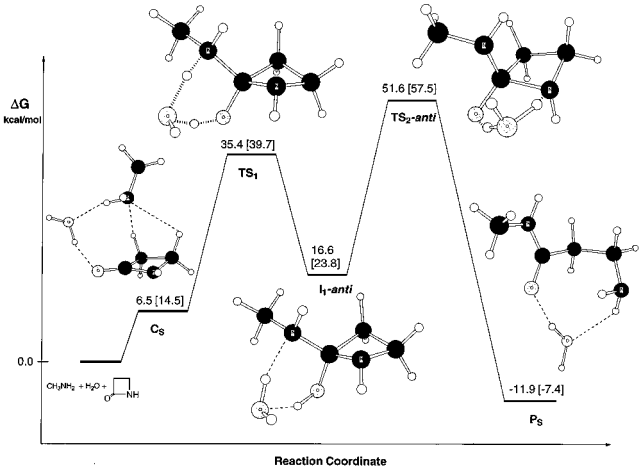

Figure 3. Gibbs energy profiles (kcal/mol) both in the gas phase and in solution (in brackets) for the anti stepwise reaction channel corresponding to the H_2O-assisted aminolysis reaction of 2-azetidinone.

6-31G** $\Delta\Delta G_{\text{solvation}}$ terms obtained with the Nancy model to $\Delta G_{\text{gas phase}}$ gives $\Delta G_{\text{solution}}$ in Table 1. We note that these $\Delta G_{\text{solution}}$ figures compare directly with those previously obtained for the thermal and RNH_2-assisted aminolysis of 2-azetidinone.[9−11] Figure 2 shows the corresponding Gibbs energy profile for the concerted mechanism while Figures 3 and 4 represent the Gibbs energy profiles for the *anti* and the *syn* stepwise mechanisms, respectively.

(a) Concerted Mechanism. The prereactive complex, $\mathbf{C_C}$ in Figure 2, is 6.4 kcal/mol more stable than separate reactants in G2(MP2,SVP) electronic energy, and presents the CH_3NH_2 bound to 2-azetidinone through weak CH···O (≈2.8−3.0 Å) and CH···N (≈2.3 Å) contacts while the catalytic water molecule connects the amino group of methylamine with the amidic N atom of 2-azetidinone via NH···O and OH···N H-bonds of around 2.1 Å. When including the thermodynamic corrections this $\mathbf{C_C}$ becomes less stable than reactants (see Figure 2).

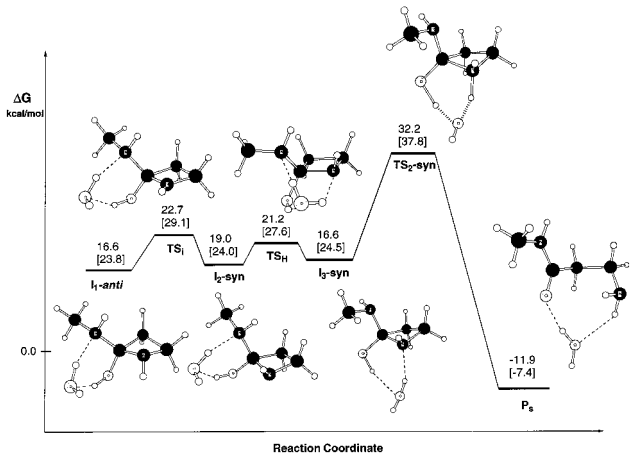

Figure 4. Gibbs energy profiles (kcal/mol) both in the gas phase and in solution (in brackets) for the evolution of the anti intermediate through the syn stepwise reaction channel corresponding to the H_2O-assisted aminolysis reaction of 2-azetidinone.

The concerted aminolysis process proceeds through a TS, $\mathbf{TS_C}$ in Figures 1 and 2, which presents a forming C−N bond (≈1.6 Å) shorter than the endocyclic breaking C−N bond (≈1.7 Å) while the water molecule mediates the H-transfer between the attacking and the forming amino groups. The calculated ΔG values for $\mathbf{TS_C}$ are 41.1 and 45.0 kcal/mol in the gas phase and in solution, respectively. The corresponding product complex, $\mathbf{P_C}$ in Figure 2, has $\Delta G_{\text{gas phase}}$ and $\Delta G_{\text{solution}}$ values of −9.4 and −3.5 kcal/mol, respectively.

(b) Stepwise Mechanism. The corresponding prereactive complex, $\mathbf{C_S}$ in Figure 3, is 10.7 kcal/mol more stable than reactants in terms of G2(MP2,SVP) electronic energy, and presents a weak H-bond between methylamine and a CH_2 group of 2-azetidinone while the water molecule forms a OH···O H-bond with the carbonylic O atom.

$\mathbf{C_S}$ is connected with a TS, $\mathbf{TS_1}$, for the addition of one N−H bond of amine across the C−O double bond of 2-azetidinone assisted by H_2O, in which the attacking amine presents a *syn*periplanar orientation with respect to the endocyclic N lone pair. At $\mathbf{TS_1}$, the formation of the C−N bond is almost completed (≈1.5 Å) whereas the H-shift from the attacking amine to the forming hydroxyl group is much less advanced (see Figure 1). This TS determines a Gibbs energy barrier of 35.4 and 39.7 kcal/mol in the gas phase and in solution, respectively. $\mathbf{TS_1}$ evolves to give a neutral tetrahedral intermediate $\mathbf{I_1}$-***anti*** in which the hydroxyl group and the lone pair of the endocyclic N atom present an *anti*periplanar orientation (see Figure 3). In this *anti*periplanar intermediate, the catalytic water molecule is linked to the nucleophile−substrate moiety through two typical OH···O and OH···N H-bonds. Nevertheless, $\mathbf{I_1}$-***anti*** remains clearly less stable than reactants by 16.6 ($\Delta G_{\text{gas phase}}$) and 23.8 kcal/mol ($\Delta G_{\text{solution}}$). This first step is common to both stepwise mechanisms (*anti* and *syn*).

In the *anti* stepwise mechanism $\mathbf{I_1}$-***anti*** may evolve through a TS for the H-shift from the hydroxyl group to the endocyclic N atom mediated by the H_2O molecule, $\mathbf{TS_2}$-***anti*** in Figure 1. Given that in $\mathbf{TS_2}$-***anti*** the orientation of the hydroxyl group remains *anti*periplanar with respect to the endocyclic N lone pair, the H-shift proceeds between the two faces of the ring. $\mathbf{TS_2}$-***anti*** has high ΔG values of 51.6 and 57.5 kcal/mol in the gas phase and in solution, respectively. Along the reaction coordinate from $\mathbf{TS_2}$-***anti***, the C−N bond is completely broken to give a product complex $\mathbf{P_S}$ (see Figure 3) and a notable reaction energy is released. $\mathbf{P_S}$ is 11.9 ($\Delta G_{\text{gas phase}}$) and 7.4 kcal/mol ($\Delta G_{\text{solution}}$) more stable than reactants. The $\mathbf{P_S}$ conformer is around 2.5−4.0 kcal/mol more stable than $\mathbf{P_C}$. According to the above figures the rate determining TS in the *anti* stepwise mechanism is $\mathbf{TS_2}$-***anti***.

Alternatively, in the *syn* stepwise mechanism the intermediate $\mathbf{I_1}$-***anti*** can undergo easily a lone pair inversion on the endocyclic N atom through $\mathbf{TS_i}$ with an energy barrier of 6.1 ($\Delta G_{\text{gas phase}}$) and 5.3 kcal/mol ($\Delta G_{\text{solution}}$) with respect to $\mathbf{I_1}$-***anti***, to give a second conformer $\mathbf{I_2}$-***syn***, 2.4 (gas phase) and 0.2 (solution) kcal/mol less stable. A subsequent rearrangement of the intermolecular H-bonds in $\mathbf{I_2}$-***syn*** through a TS, $\mathbf{TS_H}$, 2.2 (gas-phase) and 3.6 (solution) kcal/mol above $\mathbf{I_2}$-***syn***, yields a third conformer $\mathbf{I_3}$-***syn*** that is practically isoenergetic to $\mathbf{I_1}$-***anti*** (see Figure 4). From $\mathbf{I_3}$-***syn*** the ring opening of the β-lactam ring can take place through $\mathbf{TS_2}$-***syn***. As a result of the *anti/syn* isomerization though $\mathbf{TS_i}$, the H-shifts take place now over one face of the ring. The $\Delta G_{\text{gas phase}}$ and $\Delta G_{\text{solution}}$ values of $\mathbf{TS_2}$-***syn*** are 32.2 and 37.8 kcal/mol, respectively. Figure 4 shows that the activation energies required for either reversing to reactants or cleaving the tetrahedral intermediates lie in the range 13−19 kcal/mol both in the gas phase and in solution. These values are much larger than those for the *anti/syn* isomerization process and, therefore, the $\mathbf{I_1}$-***anti*** and $\mathbf{I_3}$-***syn*** species could be considered as relatively stable intermediates in rapid mutual interconversion. It may be interesting to note that previous work[11] has shown that these neutral intermediates for the aminolysis of 2-azetidinone are also much more stable species against fragmentation into reactants than *zwitterionic* intermediates.

The Gibbs energy profiles shown in Figures 2−4 predict clearly that the *syn* stepwise route for the water-assisted aminolysis of 2-azetidinones is the most favored mechanism. In effect, the rate-determining TS of this mechanism, $\mathbf{TS_1}$, is around 5−6 and 16−18 kcal/mol more stable than $\mathbf{TS_C}$ and the rate-determining TS of the *anti* stepwise mechanism, $\mathbf{TS_2}$-***anti***, respectively, both in the gas phase and in solution.

(c) The Catalytic Role of Water. Comparing the energy barrier for the most favorable mechanism presented above with the corresponding energy barrier for the noncatalyzed process,[9] we see that the catalytic action of one water molecule amounts to 23.0 kcal/mol in G2(MP2,SVP) electronic energy and to 12.6 and 9.1 kcal/mol in Gibbs energy in the gas phase and in solution, respectively, despite the entropic destabilization. Hence, a purely uncatalyzed mechanism for the aminolysis reaction of monocyclic β-lactams in aqueous solution would not be a competitive process with respect to the water-assisted mechanism.

We have previously reported[10,11] that in all the TSs for the amine-assisted aminolysis processes the catalyst presents a clear cationic character of methylammonium in consonance with amine basicity. In contrast, the ancillary water molecule in the water-assisted aminolysis of 2-azetidinone presents a variable character depending on the TS considered. We see from bond distances and atomic charges in Figure 1 that at $\mathbf{TS_C}$ the catalytic water molecule presents an appreciable hydroxide character. At $\mathbf{TS_1}$ the catalytic moiety presents an intermediate character between OH^- and H_2O. At $\mathbf{TS_2}$-***anti*** the catalytic moiety presents an intermediate character between H_2O and H_3O^+. Finally the catalyst presents a certain hydroxide character at $\mathbf{TS_2}$-***syn***, slightly less accentuated than that at $\mathbf{TS_C}$. A similar picture is obtained by a B3LYP/6-31G** configurational analysis of the TSs carried out assuming three different fragment partitions (see Table 2). In effect, we see in Table 2 that the water-assisted TSs are considerably more complex than the amine-assisted ones in the sense that they are always a mixture

Table 2. Coefficients of Zero Configuration C_{AB} Calculated by Means of a B3LYP/6-31G** Configuration Analysis of the Main TSs Assuming Different Fragment Partitions AB

	C_{AB}			
fragment partition	**TS_C**	**TS_1**	**TS_2-*anti***	**TS_2-*syn***
A = OH^-	0.562	0.529	0.408	0.538
B = 1,1-dimethylamino-alkoxy cation				
A = H_2O	0.539	0.548	0.547	0.524
B = neutral 1,1-dimethylamino-alcohol				
A = H_3O^+	0.481	0.491	0.552	0.418
B = 1,1-dimethylamino-alkoxy anion				

of two electronic partitions in which the water molecule may appear as OH^-, H_2O, or H_3O^+ owing to its amphoteric character. This flexibility of the water molecule appears to play an important role in its catalytic action.

Comparing the relative energies in Table 1 with figures corresponding to the amine-assisted process,[11] we see that for the concerted mechanism in the gas phase the energetic catalytic effect of water is 5.9 kcal/mol greater than that of one amine molecule. At **TS_1** and **TS_2-*syn*** the stabilization gained by the assistance of one water molecule in the gas phase is 3.8 and 4.9 kcal/mol greater, respectively, than that by one amine molecule. In contrast, at **TS_2-*anti*** the amine-assisted structure is 7.0 kcal/mol more favorable. These energetic differences correlate well with the fragment partition described above: the more positively charged the catalyst in a TS, the more favorable the amine-assisted structure. In all cases the entropic factor favors the water-assisted structures by 1−2 kcal/mol owing to their lower compactness corresponding to less bound protons. On the other hand, solvent stabilizes preferentially amine-assisted structures because of their more ionic character. Particularly, the energy barrier in aqueous solution for the most favorable mechanism (**TS_1**) is 2.5 kcal/mol lower when water is the catalyst than that of the amine-assisted process (3.8 kcal/mol in the gas phase).

Water-Assisted Aminolysis Reaction of 3α-Carboxypenam To model the specific role of solvent in the aminolysis of bicyclic β-lactam antibiotics, we investigated the water-assisted reaction between methylamine and the 3α-carboxypenam anion. Given the size and the negative charge of this β-lactam, we decided to study this process using the B3LYP/6-31+G* level of theory which includes diffuse functions to better describe this anionic system.

To asses the suitability of the B3LYP/6-31+G* methodology, we investigated the water-assisted ammonolysis of an amidic bond in a negatively charged prototype system (2-formamide-acetate). This small model system has a carboxylate group and the same connectivity as the corresponding moiety in the 3α-carboxypenam. Two mechanisms were analyzed: a concerted and a stepwise route which are very similar to those thoroughly discussed below for the aminolysis of the 3α-carboxypenam anion (see Scheme 3 and Supporting Information). Single-point G2(MP2,SVP) calculations on MP2/6-31+G* geometries and B3LYP/6-31+G* optimizations render similar relative energies for the ammonolysis of 2-formamide-acetate. Thus, the B3LYP/6-31+G* energy barriers corresponding to a TS for the concerted reaction (**TS_C-test**) and a TS for the breaking of the amidic bond in the stepwise mechanism (**TS_b-test**) are respectively 1.5 and 0.1 kcal/mol lower than the G2(MP2,SVP) ones. On the other hand, the B3LYP/6-31+G* energy barriers corresponding to a TS for the initial nucleophilic attack in the stepwise mechanism (**TS_1-test**) and a TS for a H-shift (**TS_s-test**) are 2.0 and 4.0 kcal/mol higher than the G2(MP2,SVP) values, respectively. With respect to the reaction energy of this process,

Scheme 3

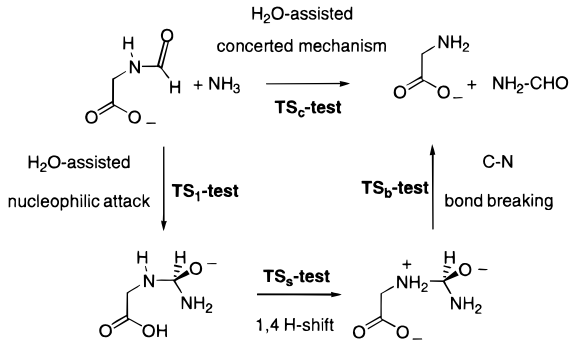

Table 3. Relative Energies (kcal/mol) with Respect to Reactants of the Structures Considered in the Aminolysis Reaction of 3α-Carboxypenam Assisted by H_2O

structures	B3LYP/6-31+G*[a]	$\Delta G_{\text{gas phase}}$[b]	$\Delta\Delta G_{\text{solvation}}$[c]	$\Delta G_{\text{solution}}$
H_2O + CH_3NH_2 + 3α-carboxypenam	0.0	0.0	0.0	0.0
C-PNC	−18.5	−0.8	27.8	27.0
TS_C-PNC	22.9	45.0	9.4	54.4
TS_1-PNC	8.5	31.0	19.8	50.7
I-PNC	3.4	24.2	22.7	46.9
TS_2-PNC	4.2	25.1	33.2	58.3
P-PNC	−43.8	−24.2	21.2	−3.0
H_2O + penicilloyl	−31.7	−20.9	7.7	−13.2

[a] Including ZPVE correction from B3LYP/6-31+G* frequencies. [b] Using B3LYP/6-31+G* electronic energies and thermal corrections. [c] Relative $\Delta G_{\text{solvation}}$ with respect to reactants from single-point B3LYP/6-31+G* PCM-UAHF calculations.

the B3LYP/6-31+G* value is only 1.5 kcal/mol below that estimated at G2(MP2,SVP). Overall, we conclude that B3LYP/6-31+G* can be a reasonable level of theory to study the water-assisted aminolysis of the 3α-carboxypenam anion although the stability of a concerted TS could be moderately overestimated at this level. Taking into account the energetic bounds defined by this calibration process, the ΔG energies obtained for the aminolysis of 2-azetidinone and 3α-carboxypenam using G2(MP2,SVP) and B3LYP/6-31+G* electronic energies, respectively, can be compared semiquantitatively.

Assuming a less sterically hindered attack of methylamine, two different mechanisms were found for this process: a concerted one and a stepwise route (inversion on the endocyclic N atom is now impeded). The resultant molecular geometries for the critical structures located on the B3LYP/6-31+G* PES are shown in Figure 5 while their corresponding relative electronic energies and Gibbs energies both in the gas phase and in solution are collected in Table 3.

Both mechanisms start from a prereactive complex **C-PNC** in which the water molecule presents a strong H-bond interaction[27] with the carboxylate group. In this complex the amine molecule is placed on the less hindered face of the 3α-carboxypenam forming two typical H-bond interactions with the O atom of H_2O and with the H atom of the bridge C atom of the bicyclic system. In terms of electronic energy including the ZPVE correction, **C-PNC** is 18.5 kcal/mol more stable than reactants (0.8 kcal/mol in terms of $\Delta G_{\text{gas phase}}$).

The concerted mechanism proceeds through **TS_C-PNC** in which the water molecule catalyzes the H-transfer from the nucleophilic methylamine to the N atom in the β-lactam ring (see Figure 5). **TS_C-PNC** presents a forming C−N bond quite

(27) Gerlt, J. A.; Kreevoy, M. M.; Cleland, W. W.; Frey, P. A. *Chem. Biol.* **1997**, 4, 259−267.

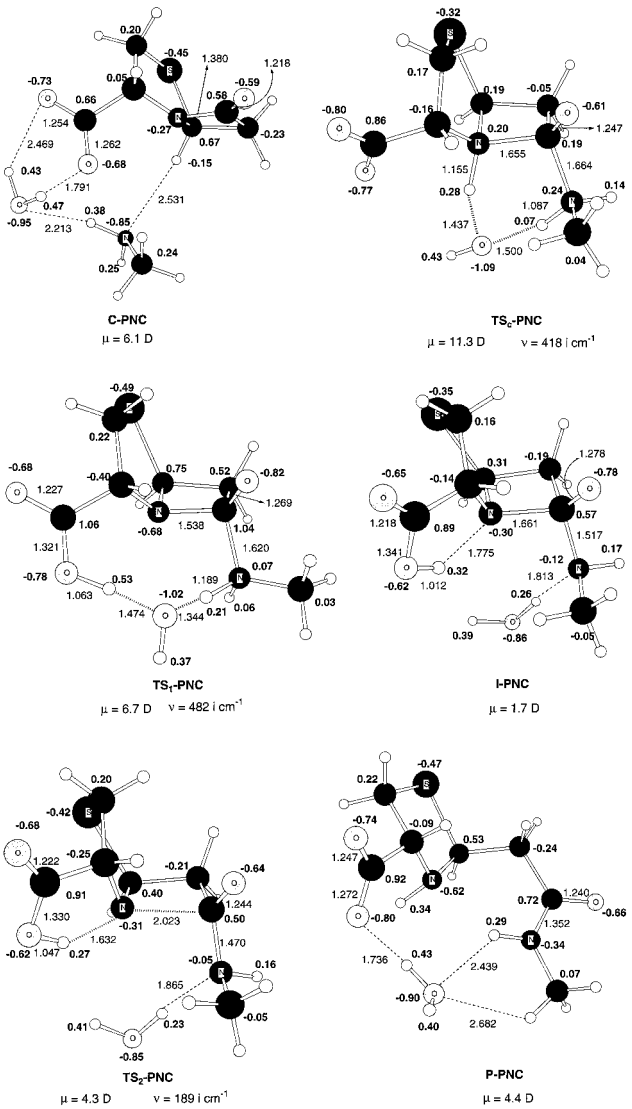

Figure 5. B3LYP/6-31+G* optimized structures for the H_2O-assisted reaction between methylamine and 3α-carboxypenam. Distances in Å. B3LYP/6-31+G* MKS atomic charges in bold characters (H atoms of the methyl group summed into the C atom). Gas-phase dipole moments (in Debyes) and frequencies corresponding to the transition vectors are also displayed.

advanced (1.664 Å), an endocyclic C−N bond barely cleaved (1.655 Å) and the two H atoms being transferred located near the amino N atoms. Thus in **TS$_C$-PNC** the catalytic moiety exhibits an accentuated hydroxide character while the amine fragment has not yet transferred a proton (N−H distance equal to 1.087 Å) and presents a MKS positive charge of +0.5 e. The $\Delta G_{\text{gas phase}}$ for **TS$_C$-PNC** with respect to separate reactants is 45.0 kcal/mol. From $\Delta G_{\text{gas phase}}$ data in Tables 1 and 3, we see that the presence of the thiazolidine ring seems to destabilize the concerted route by at least 4 kcal/mol.

In the stepwise mechanism, we found that the negatively charged carboxylate group in 3α-carboxypenam may shuttle the H atom required to form and, subsequently, cleave a tetrahedral intermediate.[28] This mechanism proceeds initially through a TS, **TS$_1$-PNC**, in which the nucleophilic attack of CH_3NH_2 takes place with simultaneous H-transfer to the carboxylate group assisted by the ancillary water molecule (see Figure 5). At **TS$_1$-PNC** the forming C−N bond is quite advanced (1.620 Å, similar to that for **TS$_C$-PNC**) and the catalytic moiety presents a certain hydroxide character. The nucleophilic amine fragment presents a positive charge of +0.4 e. In the gas phase, **TS$_1$-PNC** is much more stable than **TS$_C$-PNC**, and has a $\Delta G_{\text{gas phase}}$ value of 31.0 kcal/mol. **TS$_1$-PNC** is connected with an amino-alcoholate intermediate **I-PNC** that is 24.2 kcal/mol less stable than reactants in terms of $\Delta G_{\text{gas phase}}$. In **I-PNC** the endocyclic C−N bond has a bond distance of 1.661 Å and the β-lactam N atom bears a negative charge of −0.3 e stabilized by means of an intramolecular strong H-bond with the carboxylic group (OH···N 1.775 Å). The catalytic water molecule in **I-PNC** is placed below the β-lactam ring solvating the exocyclic amino group via a typical H-bond. The **I-PNC** intermediate can readily evolve through a TS only 0.9 kcal/mol above it in $\Delta G_{\text{gas phase}}$, **TS$_2$-PNC** in Figure 5. At **TS$_2$-PNC** the endocyclic C−N bond is completely broken whereas the H shift from the carboxylic group to the forming amino group is at its initial stage. Hence in the gas phase **I-PNC** would be a short-life species and **TS$_1$-PNC** would be the rate-determining TS for the stepwise mechanism. We note that this mechanism is quite different from that for the nonconcerted route for the aminolysis of the monocyclic 2-azetidinone and clearly more favorable than it in the gas phase.

The product complex for this reaction is **P-PNC** in Figure 5 in which the water molecule presents a H-bond interaction with one of the oxygen atoms of the carboxylate group. **P-PNC** is 24.2 kcal/mol more stable than reactants in $\Delta G_{\text{gas phase}}$. The binding energy between the ancillary water molecule and the penicilloyl compound from 3α-carboxypenam and methylamine amounts to 3.3 kcal/mol, the ΔG_{rxn} term in the gas phase being thus −20.9 kcal/mol. Interestingly, when comparing these figures with the ΔG_{rxn} for the aminolysis of 2-azetidinone (−14.9 kcal/mol), we see that the presence of the second fused ring reinforces the exothermicity of the process in the gas phase by about 5 kcal/mol.

From the results discussed above, the most favorable mechanism for the water-assisted aminolysis reaction of 3α-carboxypenam is the stepwise one. Thus, in the gas phase and in low polar media, the nucleophilic attack of CH_3NH_2 would take place with simultaneous H-transfer to the carboxylate group assisted by the ancillary water molecule.

Solvent effects on the energy profiles for the H_2O-assisted aminolysis of 3α-carboxypenam are large and have a considerable mechanistic impact (see Table 3). When the solvation energy is taken into account, **C-PNC** becomes 27.0 kcal/mol less stable than reactants. **TS$_C$-PNC**, in which both the carboxylate group and the carbonylic O atom polarize the solvent continuum (see dipole moment and atomic charges in Figure 5), is the most stabilized structure in solution with respect to reactants, having a $\Delta G_{\text{solution}}$ barrier of 54.4 kcal/mol. Since the negative charge in each of the critical structures constituting the stepwise reaction coordinate is substantially delocalized, the $\Delta G_{\text{solution}}$ values for **TS$_1$-PNC**, **I-PNC**, and **TS$_2$-PNC** (50.7, 46.9, and 58.3 kcal/mol, respectively) are much greater than the gas-phase values by 19.8, 22.7, and 33.2 kcal/mol, respectively. The product complex, **P-PNC**, is considerably disfavored by solvation and presents a $\Delta G_{\text{solution}}$ of −3.0 kcal/mol.

According to the estimated $\Delta G_{\text{solution}}$ values, the cleavage of the **I-PNC** in strong polar media would become the rate-determining step in the stepwise mechanism with a $\Delta G_{\text{solution}}$ 3.9 kcal/mol greater than that for the concerted route. Of course, in view of the moderate preferential overstabilization of the concerted mechanism at the B3LYP/6-31+G* theory level

(28) A similar mechanism has been described by Wolfe for the water-assisted methanolysis of 3α-carboxypenam at the AM1 level: Wolfe, S. *Can. J. Chem.* **1994**, *72*, 1014−1031.

(see above), the actual energy difference could be smaller. Nevertheless, further support to the kinetic preference for the concerted mechanism stems from the fact that the nucleophile at **TS_C-PNC** resembles a methylammonium structure in agreement with the reported positive Brønsted β value for the uncatalyzed reaction of benzylpenicillin with a series of amines.[6] In contrast, the structure of **TS_2-PNC**, which is the rate determining TS for the stepwise mechanism in aqueous solution, is not able to rationalize the reported Brønsted β value. Thus, theoretical results suggest that the concerted route can be the most favored mechanism for the thermal aminolysis of penicillins assisted by an ancillary water molecule in aqueous solution, in contrast with earlier proposals.[5,6]

At this point, it may be interesting to emphasize again the 2-fold role played by the carboxylate group in the theoretically proposed mechanisms for the water-assisted aminolysis of the penicillin model 3α-carboxypenam. On one hand, the carboxylate group functions as a proton acceptor/donor in the stepwise mechanism and clearly favors the aminolysis process in the gas phase. On the other one, its negative charge reinforces preferentially the solute−solvent electrostatic interactions at the TS for the concerted mechanism. Similar results have been found in the case of the amine-assisted aminolysis reaction of 3α-carboxypenam.[12]

Aminolysis Reaction between β-Lactams and HSA: The Lys_{199} Active Center Computational model systems are very valuable approaches to understanding biological catalysis in terms of the energies and geometries of TSs and intermediates of reactions of small systems relative to enzymatic substrates and catalysts.[29] To find out if our results on the aminolysis reaction of model systems may render some insight into the reaction of β-lactams with HSA, the crystallographic structure of HSA[13] and experimental observations on HSA-penicillin binding processes[30] are discussed at this point. On the basis of these data, the protonation state of the key residue Lys_{199} as well as some mechanistic details concerning the aminolysis reaction of benzylpenicillin with the ϵ-amino group of Lys_{199}, will be addressed.

(a) Structure of HSA and HSA-Penicillin Binding Processes. Two independent X-ray structure determinations of the native HSA to a resolution of 2.5 and 2.8 Å, respectively, have been published.[13] Both structures have two protein molecules per asymmetric unit, and hence there are now four observations of the structure of HSA showing a satisfactory overall agreement. The 585 amino acid HSA molecule is heart-shaped and consists of three repeating domains (labeled I−III), each of which is divided into two subdomains (A−B). The protein has a high α-helical content (67%) and a large number of disulfide bonds (17). Previous studies have shown that the principal binding regions in HSA are located in subdomains IIA and IIIA.[13,30] These binding pockets in HSA have a greater affinity for small, negatively charged hydrophobic molecules such as aspirin, *p*-nitrophenylacetate, triodobenzoic acid, etc. More specifically, residues Trp_{214}, Tyr_{411}, and Lys_{199}, which have been implicated in various binding processes, are located strategically in the IIA or IIIA hydrophobic pockets.

To further understand either the molecular mechanisms of interactions of small molecules with biomolecules or the origin of penicillin allergy, the formation of complexes between HSA and various penicillins has been investigated thoroughly by experiment.[3,30] On one hand, HSA and penicillins form relatively weak complexes stabilized by electrostatic interactions and hydrophobic effects. For these weak complexes, NMR experiments and indirect observations for a series of penicillins indicate that penicillins mainly interact with HSA through both the benzene ring of the lipophilic chain and the carboxylate group.[30] On the other hand, HSA and penicillins can also bind covalently via the aminolysis reaction between the β-lactam ring and ϵ-amino groups rendering penicilloyl-containing peptides in different binding regions of HSA that involve several lysine residues (particularly with Lys_{199}).[3] Most importantly, these penicilloyl−albumin complexes, which have no antibacterial activity, constitute the major antigenic determinant of penicillin allergy.

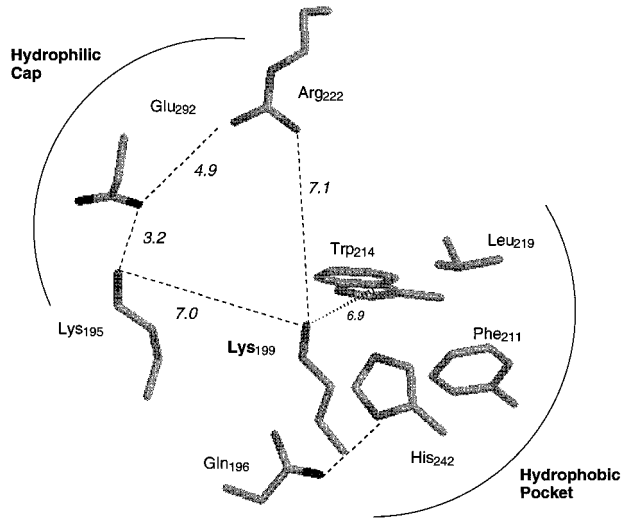

Figure 6. The environment of the Lys_{199} binding site in HSA as obtained directly from X-ray refinement. Distances in Å.

Figure 6 shows a three-dimensional representation of the side chains of the residues constituting the closer environment of Lys_{199} as obtained directly from X-ray refinement.[13b] This binding site of HSA, which is located in its IIA subdomain, shows a hydrophobic pocket (Phe_{211}, Leu_{219}, Trp_{214}) capped by hydrophilic or polar residues (Gln_{196}, His_{242}, Arg_{222}, Lys_{195}, Glu_{292}). The key residue, Lys_{199}, is situated in the vicinity of the hydrophobic pocket, its side chain pointing toward the entrance channel of the binding crevice. Although the resolution of the reported crystal structures of HSA (2.5−2.8 Å) has not allowed the determination of the water content of this binding site, it is reasonable to expect that some water molecules could be bound by means of H-bond contacts with the most polar residues making up the hydrophilic cap of the binding site.

(b) Protonation State of Lys_{199}. Clearly the overall protonation state of the Lys_{199} binding site will determine the fundamental mechanisms for the aminolysis reaction of benzylpenicillin or other substrates with HSA. Thus, the critical feature of the most likely mechanisms requires Lys_{199} to be deprotonated to facilitate the nucleophilic attack of the reactive amino group toward the carbonylic C atom of β-lactam rings. Interestingly, a neutral protonation state for Lys_{199} has been supported by experimental results[31,32] observing HSA modifications due to the nonenzymatic reaction of glycosil and arylating reagents with exceptionally nucleophilic lysine residues as Lys_{199}. This chemical behavior is consistent with an unusually low pK_a of 7.9 for Lys_{199} which therefore exists in its neutral form. The

(29) Tantillo, D. J.; Chen, J.; Houk, K. N. *Curr. Opin. Chem. Biol.* **1998**, *2*, 743−750 and references therein.

(30) Landau, M. *Russ. J. Org. Chem.* **1969**, *34*, 615−628.

(31) (a) Gerig, J. T.; Reinheimer, J. D. *J. Am. Chem. Soc.* **1975**, *97*, 168−173. (b) Gerig, J. T.; Katz, K. E.; Reinheimer, J. D. *Biochim. Biophys. Acta* **1978**, *534*, 196−209.

(32) Iberg, N.; Fluckiger, R. *J. Biol. Chem.* **1986**, *261*, 13542−13545.

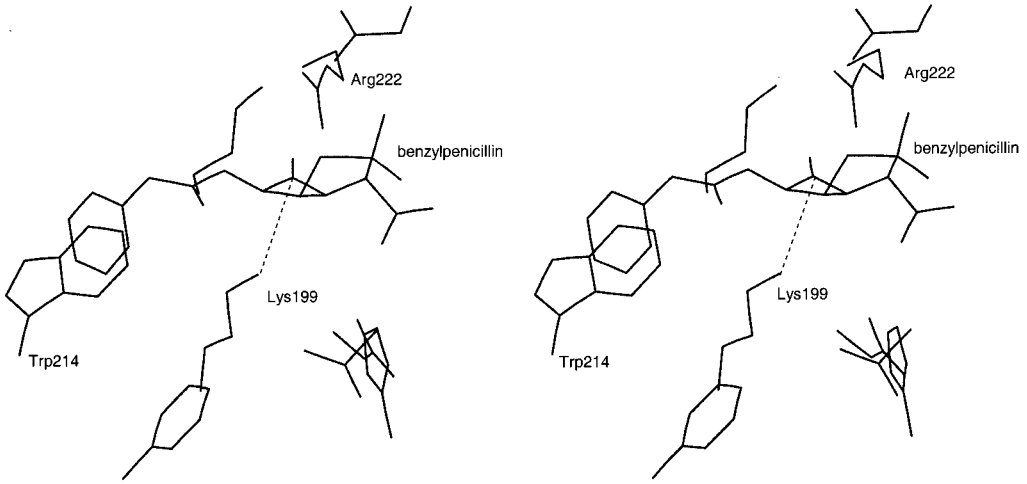

Figure 7. Stereoscopic representation of the Lys_{199} binding site in HSA including a benzylpenicillin substrate.

Scheme 4

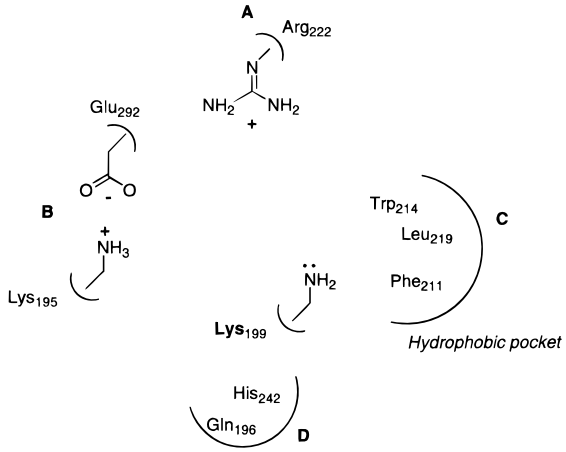

X-ray structure may explain this since Lys_{199} appears in close proximity to other plausibly charged residues such as Arg_{222} and Lys_{195} in Figure 6. Scheme 4 shows a hypothetical charge distribution of the Lys_{199} binding site which bears globally a unit positive charge, the Lys_{199} amino group being deprotonated. Moreover, we assume in Scheme 4 that the unit positive charge is delocalized along the conjugated skeleton of Arg_{222} while the Glu_{292} and Lys_{195} form an ionic pair presumably stabilized by water molecules surrounding the hydrophilic cap. This seems to be the simplest proposal in agreement with experimental evidence (see above).

To test the hypothetical model displayed in Scheme 4, we carried out single-point ab initio and semiempirical calculations on some molecular models of the Lys_{199} binding site built from X-ray crystallographic coordinates,[13b] the H atoms being added by molecular modeling. Table 4 collects the contribution of HF/6-31G* electronic energies to the proton affinity (PA) of the Lys_{199} amino group as evaluated in different molecular environments derived from that depicted in Scheme 4. At the HF/6-31G* level, the electronic PA of Lys_{199} within the full model amounts to 196 kcal/mol. However, removal of the positively charged Arg_{222} residue increases this value dramatically (233 kcal/mol). Table 4 indicates that other residues have a moderate influence: the exclusion of the $Gln_{292}^{-}/Lys_{195}^{+}$ ionic pair increases by 12 kcal/mol the PA of Lys_{199} whereas the omission of the His_{242}/Gln_{296} pair and the hydrophobic pocket decreases it by only 2 and 6 kcal/mol, respectively. Similar trends are observed at the PM3 and AM1 semiempirical levels although

Table 4. Contribution of Electronic Energies to the Proton Affinity of the Lys_{199} Side Chain in the Model System Shown in Figure 6 (see group notation in Scheme 4)[a]

system	HF/6-31G*	PM3	AM1
full model	196	163	128
full model except **A**	233	200	165
full model except **B**	208	168	135
full model except **C**	194	155	123
full model except **D**	191	153	120
isolated Lys_{199} side chain	233	200	165

[a] Single-point HF/6-31G* and semiempirical calculations were carried using the X-ray crystallographic coordinates augmented with the inclusion of standard hydrogen atoms.

the PM3 parametrization renders absolute PA much closer to the HF/6-31G* ones than the AM1 method. Comparing the HF/6-31G* PA estimations with that of the isolated Lys_{199} (233 kcal/mol),[33] we confirm that, in effect, the specific effect of the charged residue Arg_{222} can reduce very importantly the intrinsic basicity of the Lys_{199} amino group embedded in the IIA binding site in HSA. Therefore, the structural analyses[13] complemented by our calculations are in consonance with the experimentally reported[31,32] substantial lowering of the pK_a for Lys_{199} in HSA.

(c) Reaction Mechanism between Benzylpenicillin and Lys199 in HSA. Figure 7 shows that benzylpenicillin may bind noncovalently to the binding site in a favorable orientation to initiate the aminolysis reaction.[34] This particular orientation could be stabilized by $\pi-\pi$ interactions between the phenyl group of benzylpenicillin and the Trp_{214} residue in the hydrophobic pocket of the binding site while the neutral amino group of Lys_{199} is favorably oriented toward the least hindered face of benzylpenicillin, having a N(Lys_{199})-C(BP) contact of $\approx$3.5 Å. We also see in Figure 7 that the carboxylate group of benzylpenicillin points toward the entrance channel of the binding site, i.e., it may be reasonable to expect that some water molecules, originally solvating this carboxylate group in solu-

(33) It is worth noting that geometry relaxation could have a minor influence at this point given that the electronic PA of the fully optimized *n*-butylamine at the HF/6-31G* level (233.5 kcal/mol) is practically coincident with that obtained using X-ray coordinates. Furthermore, the G2(MP2,SVP) electronic PA of *n*-butylamine (227.9 kcal/mol) compares well with the HF/6-31G* values.

(34) After having visualized some potentially reactive orientations between benzylpenicillin and our model of the Lys_{199} binding site, we selected the orientation displayed in Figure 7 which in turn was obtained after 100 PM3 cycles of geometry optimization with coordinates of the amino acid side chains constrained to their X-ray experimental values.

Scheme 5

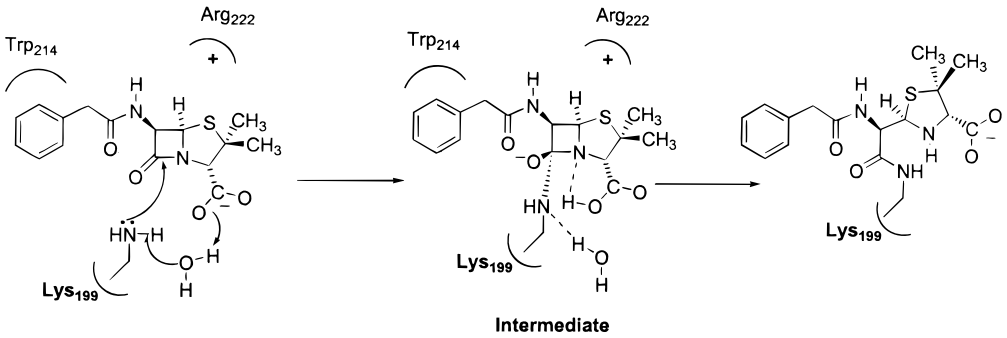

tion, can be placed around the carboxylate group and the Lys_{199} residue in a prereactive HSA−penicillin complex.

As mentioned above, the environment polarity exerts a notable influence on both the mechanistic preference and the magnitude of the activation energy for the water-assisted reaction between 3α-carboxypenam and methylamine. Assuming that the presence of the hydrophobic pocket would result in a low polarity local region around Lys_{199}, the most favored mechanism for the aminolysis reaction of benzylpenicillin in this protein environment would be analogous to the stepwise mechanism found for the water-assisted aminolysis of 3α-carboxypenam in the gas phase. In this mechanism one water molecule would mediate the H transfer between the attacking nucleophilic amino group of Lys_{199} and the carboxylate group in benzylpenicillin to form an intermediate (see Scheme 5). The cleavage of the β-lactam ring would proceed then with synchronous H shift from the carboxylic group to the endocyclic N atom of benzylpenicillin. The presence of a partial negative charge on the carbonylic O atom all along the carboxylate-mediated product channel could be stabilized by the positively charged Arg_{222} residue acting as a sort of oxyanion hole (see Scheme 5). The release of the reaction energy would lead to the practically irreversible formation of a benzylpenicilloyl group linked to the Lys_{199} amino group. Furthermore, given that the energy barrier for a water-assisted aminolysis reaction is lower in a low polar environment than in aqueous solution, the reaction between the Lys_{199} residue and penicillins would proceed in a particularly favorable way.

Conclusions

Three different mechanisms were found for the water-assisted aminolysis of 2-azetidinone: a concerted one and two stepwise routes. Both in the gas phase and in aqueous solution the most favorable mechanism is the *syn* stepwise one. In this mechanism the attack of the amine gives rise to an *anti* neutral tetrahedral intermediate, which through inversion on the N atom transforms into a *syn* intermediate before yielding the product. The rate determining step is the formation of the *anti* intermediate with a Gibbs energy barrier of 35.4 and 39.7 kcal/mol in the gas phase and in aqueous solution, respectively. In contrast with the amine-assisted aminolysis process where the catalyst presents a clear cationic character of methylamonium, the ancillary water molecule in the water-assisted process presents a variable character (between OH^-, H_2O, and H_3O^+) depending on the TS considered. The catalytic action of water in this mechanism is more efficient than that of methylamine owing to its more amphoteric character.

For the water-assisted aminolysis of the 3α-carboxypenam anion, we found a concerted and a stepwise mechanism (inversion on the endocyclic N atom is impeded). In the gas phase the stepwise mechanism is the most favorable one. The nucleophilic attack on the penicillanate to form a short-lived neutral intermediate is the rate determining step with a Gibbs energy barrier of 31.0 kcal/mol. In this mechanism one water molecule would mediate a H transfer between the nucleophile and the carboxylate group of the penicillanate, which in turn gives the H atom to the forming amino group in the second step. In aqueous solution the most favorable mechanism is the concerted one. The nucleophilic moiety in **TS_C-PNC** presents a methylammonium character in consonance with the experimentally reported Bronsted β value of 1.0. The corresponding Gibbs energy barrier is 54.4 kcal/mol, which compared with the gas-phase one indicates that the aminolysis of 3α-carboxypenam would be more effective in low polar environments.

Finally, by re-interpreting our theoretical calculations on the water-assisted aminolysis reaction of β-lactams in the context of the X-ray structure and experimental data regarding the binding ability of the Lys_{199} binding site in HSA, we propose that the most favorable mechanism for the aminolysis of benzylpenicillin in this protein environment would be analogous to the stepwise mechanism found for the water-assisted aminolysis of 3α-carboxypenam. Thus the rate determining step for the aminolysis reaction between benzylpenicillin and the Lys_{199} residue would be the nucleophilic attack of the Lys_{199} amino group with simultaneous H-transfer to the carboxylate group assisted by one water molecule. The knowledge gained on the origin of the energy barrier for the aminolysis reaction between β-lactam antibiotics and HSA could be useful to design rational strategies to develop chemically modified β-lactams without presenting allergenic reactions, but preserving their antibiotic activity.

Acknowledgment. The authors are grateful to CIEMAT for computer time on the Cray YMP and thank FICYT (Principado de Asturias) and DGESIC for financial support (PB-MAS96-23 and PB97-1300, respectively). D.S. and N.D. also thank DGESIC for their grants (EX99-10863995Z and PB98-44430549, respectively).

Supporting Information Available: Figures showing the molecular geometries for the prereactive complexes, intermediates, and products of the water-assisted aminolysis of 2-azetidinone; table with the relative energies and figures showing the molecular geometries for the water-assisted ammonolysis of the 2-formamide-acetate anion; coordinates of all the optimized structures for the water-assisted aminolysis of 2-azetidinone and 3α-carboxypenam (PDF). This material is available free of charge via the Internet at http://pubs.acs.org.

JA993547Q